Quantifying the Impact of Dynamic Storm-Time Exospheric Density on Plasmaspheric Refilling

Lara Waldrop[1], Gonzalo Cucho-Padin[1], and Naomi Maruyama[2]

[1]University of Illinois at Urbana-Champaign
[2]University of Colorado Boulder

November 21, 2022

Abstract

As soon as the outer plasmasphere gets eroded during geomagnetic storms, the greatly depleted plasmasphere is replenished by cold, dense plasma from the ionosphere. A strong correlation has been revealed between plasmaspheric refilling rates and ambient densities in the topside ionosphere and exosphere, particularly that of atomic hydrogen (H). Although measurements of H airglow emission at plasmaspheric altitudes exhibit storm-time response, temporally static distributions have typically been assumed in the H density in plasmasphere modeling. In this presentation, we evaluate the impact of a realistic distribution of the dynamic H density on the plasmaspheric refilling rate during the geomagnetic storm on March 17, 2013. The temporal and spatial evolution of the plasmaspheric density is calculated by using the Ionosphere-Plasmasphere Electrodynamics (IPE) model, which is driven by a global, 3-D, and time-dependent H density distribution reconstructed from the exospheric remote sensing measurements by NASA's TWINS and TIMED missions. We quantify the spatial and temporal scales of the refilling rate and its correlation with H densities.

Quantifying the impact of the Dynamic Storm-time Exosphere Density on Plasmaspheric Refilling

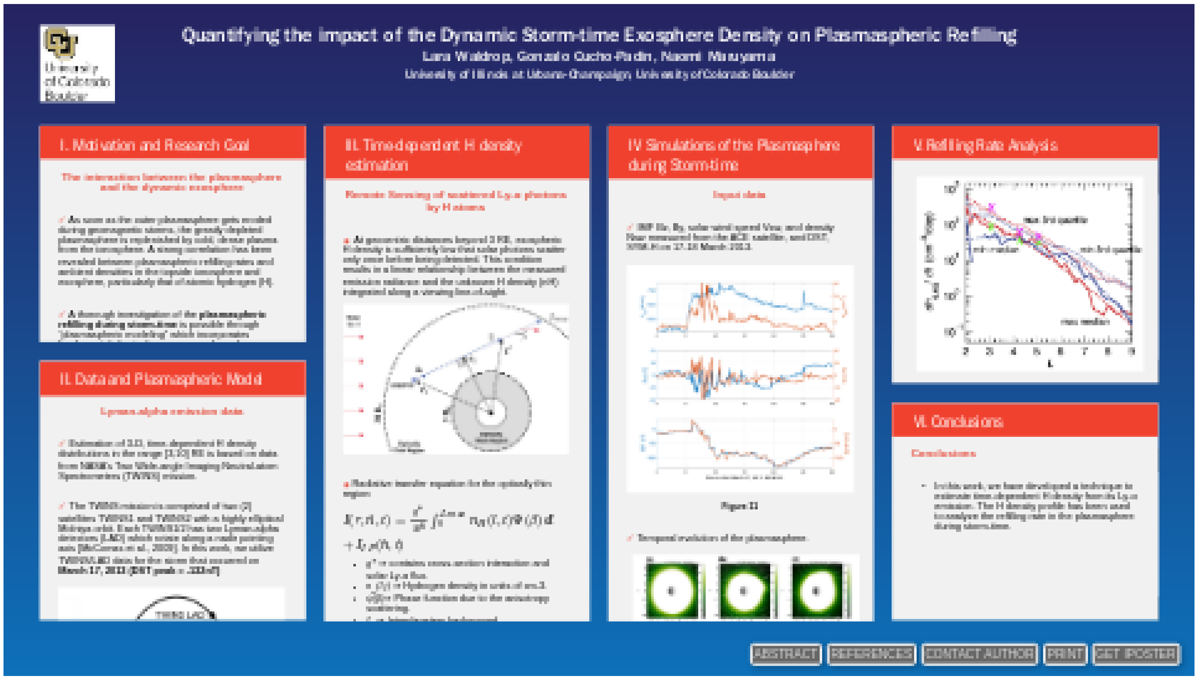

Lara Waldrop [1], Gonzalo Cucho-Padin [1], Naomi Maruyama [2]

[1] University of Illinois at Urbana-Champaign, [2] University of Colorado Boulder
Contact: gac3@illinois.edu

PRESENTED AT:

AGU FALL MEETING
Online Everywhere | 1–17 December 2020

I. MOTIVATION AND RESEARCH GOAL

The interaction between the plasmasphere and the dynamic exosphere

◉ As soon as the outer plasmasphere gets eroded during geomagnetic storms, the greatly depleted plasmasphere is replenished by cold, dense plasma from the ionosphere. A strong correlation has been revealed between plasmaspheric refilling rates and ambient densities in the topside ionosphere and exosphere, particularly that of atomic hydrogen (H) **[**Krall et al., 2018 (http://agupubs.onlinelibrary.wiley.com/doi/full/10.1002/2017SW001780)].

◉ A thorough investigation of the **plasmaspheric refilling during storm-time** is possible through "plasmaspheric modeling" which incorporates fundamental physical processes such as charge-exchange, ion-ion collisions, and wave-particle interactions. However, its accuracy **depends critically on the specification of the exospheric H density distributions.**

◉ The terrestrial exosphere is the uppermost layer of the atmosphere which extends from 500 km (exobase) up to ~30 R_E (Earth radii). The atomic hydrogen (H) is the main constituent.

◉ **Remote sensing of solar Lyman-alpha photon scattered by exospheric H atoms ("Ly-α" @ 121.6nm)** is the only means available to estimate exospheric density distributions over such a vast region.

◉ Existing theoretical and data-based H density models have been generated **specifically for quiet-time conditions** whereby the assumption of a static exosphere is likely valid.

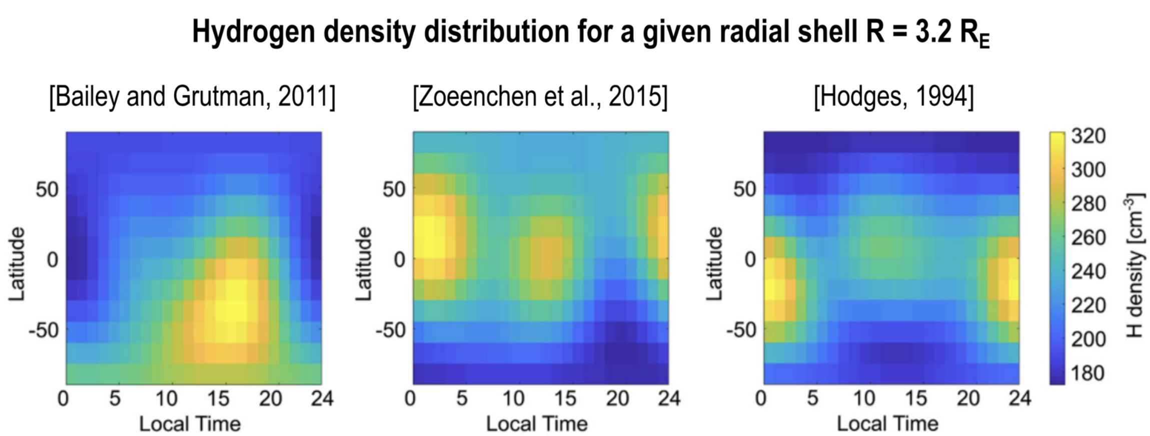

◉ Recent observations of Ly-α emission scattered by exospheric H atoms unveiled the **rapid fluctuations in their density distributions during geomagnetic storms** [Zoeenchen et al., 2017 (https://doi.org/10.5194/angeo-35-171-2017), Kuwabara et al., 2017 (https://agupubs.onlinelibrary.wiley.com/doi/full/10.1002/2016JA023247)]. Such a dynamic behavior is yet to be included in those H density models.

Scattered Lyman-alpha (@121.6nm) variation during storm time

Source: [Zoennchen et al., 2017]

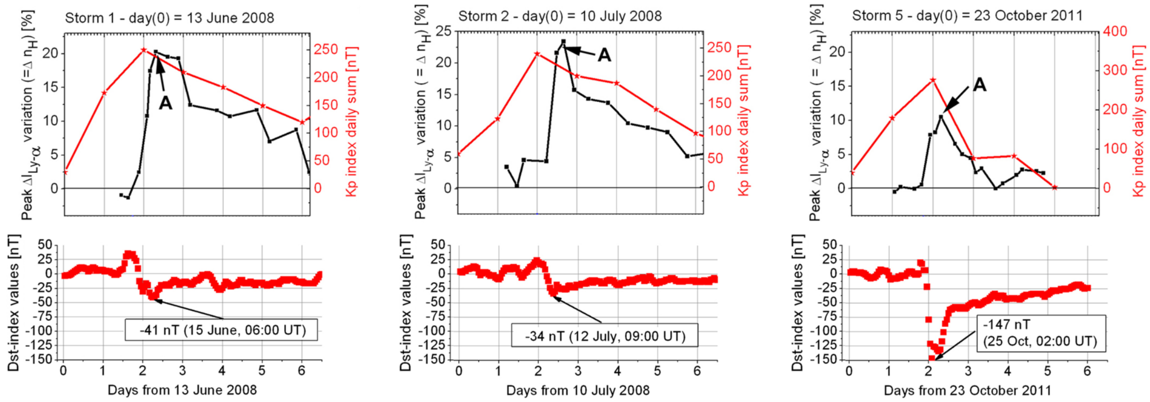

Overarching question

What is the role of the storm-time terrestrial exosphere on the plasmaspheric refilling rate?

◉ To address this question, we estimate the 3-D, time-dependent hydrogen density distributions based on its Ly-α emission and a tomographic approach during storm-time. We then include the retrieved H density profile into a plasmasphere model and assess the refilling rate.

II. DATA AND PLASMASPHERIC MODEL

Lyman-alpha emission data

Estimation of 3-D, time-dependent H density distributions is based on data from NASA's Two Wide-angle Imaging Neutral-atom Spectrometers (TWINS) mission [McComas et al., 2009 (http://doi.org/10.1007/s11214-008-9467-4)]:

- TWINS mission is comprised of two satellites TWINS1/2.
- Each satellite has two Lyman-alpha detectors (LAD1/2)
- We utilize data for the storm that occurred on **March 17, 2013 (DST peak = -132nT)**
- Estimation range: [3,12] R_E geocentric distance.

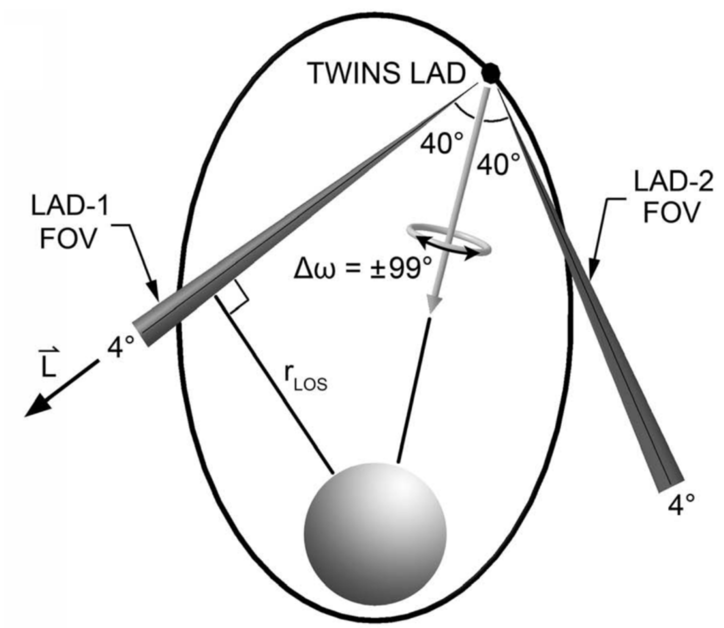

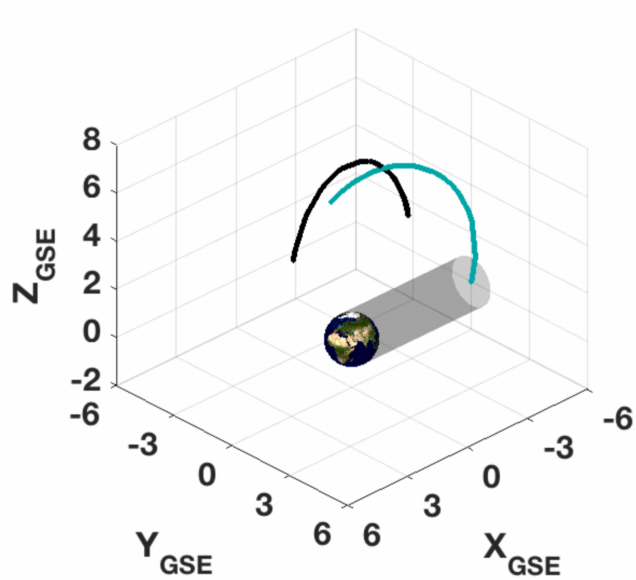

Left panel from [Bailey and Grutman, 2011 (https://doi.org/10.1029/2011JA016531)]

◉ TWINS data availability is not continuous during the day.

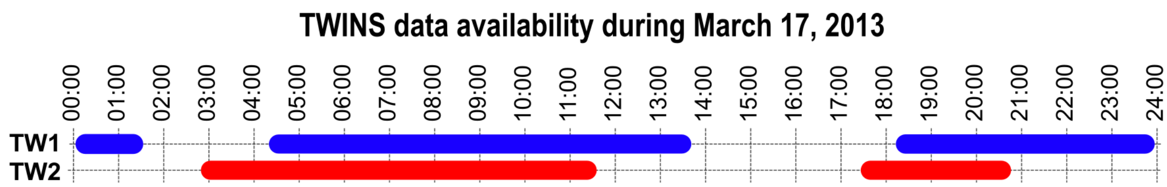

◉ Additionally, we use data from the Global UltraViolet Imager (GUVI) on-board the Thermosphere Ionosphere Mesosphere Energetics and Dynamics (TIMED) mission to estimate an averaged and spherically symmetric H density distribution during solar-maximum conditions in the region [92, 500] km [Qin et al, 2017 (https://doi.org/10.1002/2017JA024489)]

◉ We connect both datasets (GUVI and TWINS) using a two-exponential function based on a similar procedure demonstrated by [Østgaard et al., 2003 (https://doi.org/10.1029/2002JA009749)] using GEO/IMAGE data.

Plasmaspheric Model

◉ We use the Ionosphere-Plasmasphere Electrodynamics (IPE) model to simulate the plasmaspheric dynamics.

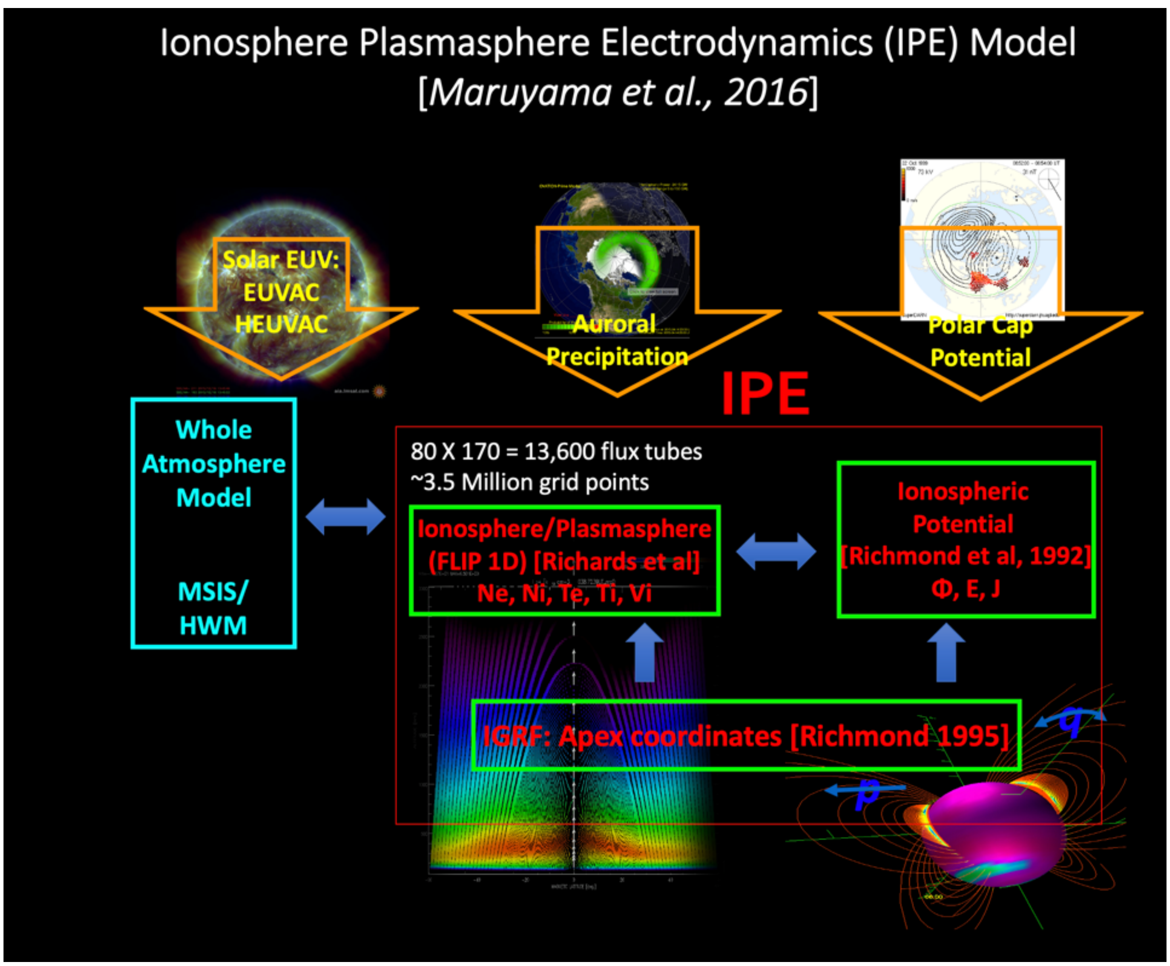

III. TIME-DEPENDENT H DENSITY ESTIMATION

Remote sensing of scattered Ly-α photons by H atoms

◉ At geocentric distances beyond 3 R_E, exospheric H density is sufficiently low that solar photons scatter only once before being detected. This condition results in a **linear relationship** between the measured emission radiance and the unknown H density (n_H) integrated along a viewing line-of-sight.

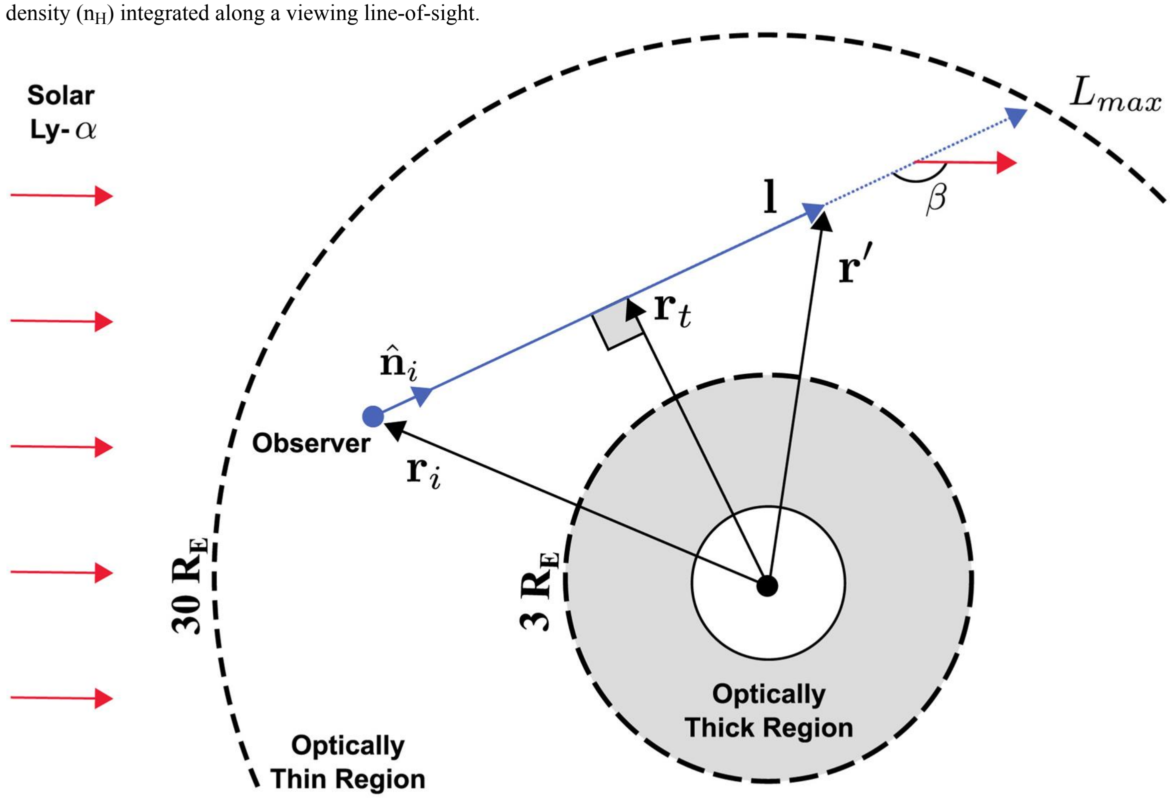

◉ Radiative transfer equation for the optically thin region:

$$I(r,\hat{n},t) = \frac{g^*}{10^6}\int_0^{Lmax} n_H(l,t)\Psi(\beta)dl + I_{IP}(\hat{n},t)$$

- g^* ⇒ contains cross-section interaction and solar Ly-α flux.
- $n_H(l,t)$ ⇒ Hydrogen density in units of cm-3.
- $\psi(\beta)$⇒ Phase function due to the anisotropy scattering.
- I_{IP}⇒ Interplanetary background.
- n_i ⇒ LOS direction.
- r ⇒ Tangential distance of a LOS.

◉ The tomographic approach states that the volume of interest should be divided into voxels with a constant H density number. In this work, we adopt Δr = 0.3125 RE, Δθ = 15 deg and Δφ = 15 deg yielding 6912 spherical voxels.

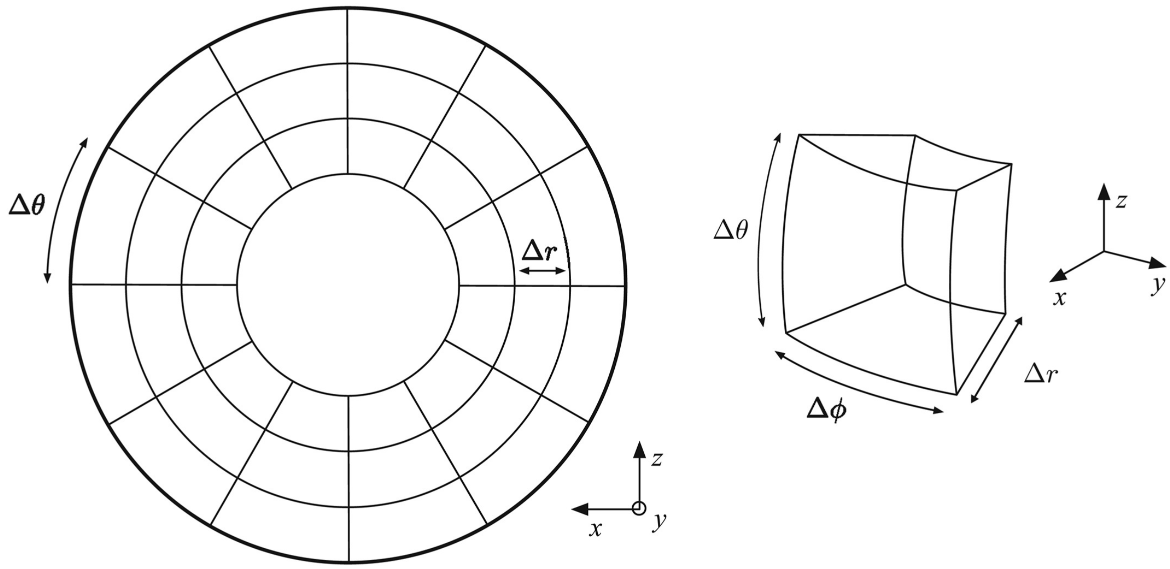

◉ After the spatial discretization into spherical voxels is performed, the radiative transfer equation adopts the form:

$$\mathbf{y} = L\mathbf{x}$$

where:

- $\boldsymbol{y}$ ⇒ (known) the measurement vector generated by I-I_{IP}
- L ⇒ (known) the observation matrix generated with LOS direction, satellite position, voxel dimension and solar Ly-α flux data.
- $\boldsymbol{x}$ ⇒ (unknown) the vector that contains the H density number per voxel.

◉ Static tomographic reconstruction $\boldsymbol{x^s}$ can be performed during quiet-time conditions using all available data and solving the expression above. During storm-time, a time-dependent model should be used: $\boldsymbol{y}_k$=$L_k\,\boldsymbol{x}_k$ such that the input data stream may generate sequential reconstructions $\boldsymbol{x^d}$ every time k.

◉ Kalman Filter has been used to estimate the 3-D, time-dependent H density distribution from Ly-α emission. We used a **two-hour period** for reconstructions.

Kalman Filter Algorithm

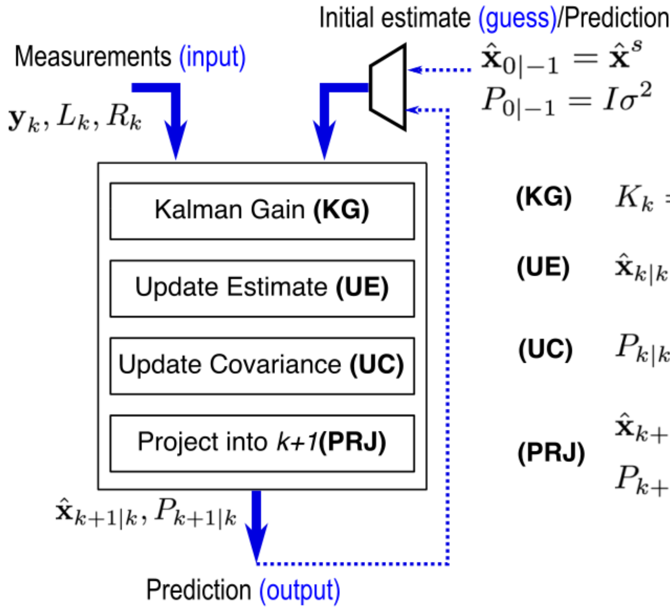

(KG) $$K_k = P_{k|k-1} L_k^T (L_k P_{k|k-1} L_k^T + R_k)^{-1}$$

(UE) $$\hat{\mathbf{x}}_{k|k} = \hat{\mathbf{x}}_{k|k-1} + K_k(\mathbf{y}_k - L_k \hat{\mathbf{x}}_{k|k-1})$$

(UC) $$P_{k|k} = P_{k|k-1} - K_k L_k P_{k|k-1}$$

(PRJ) $$\hat{\mathbf{x}}_{k+1|k} = F_{k-1}\hat{\mathbf{x}}_{k|k}$$
$$P_{k+1|k} = F_k P_{k|k} F_k^T + Q_k$$

◉ The initial estimate xs is obtained by performing a static tomographic reconstruction using TWINS data for October-December 2012 during quiet-time conditions [Cucho-Padin & Waldrop, 2018 (https://doi.org/10.1029/2018JA025323)].

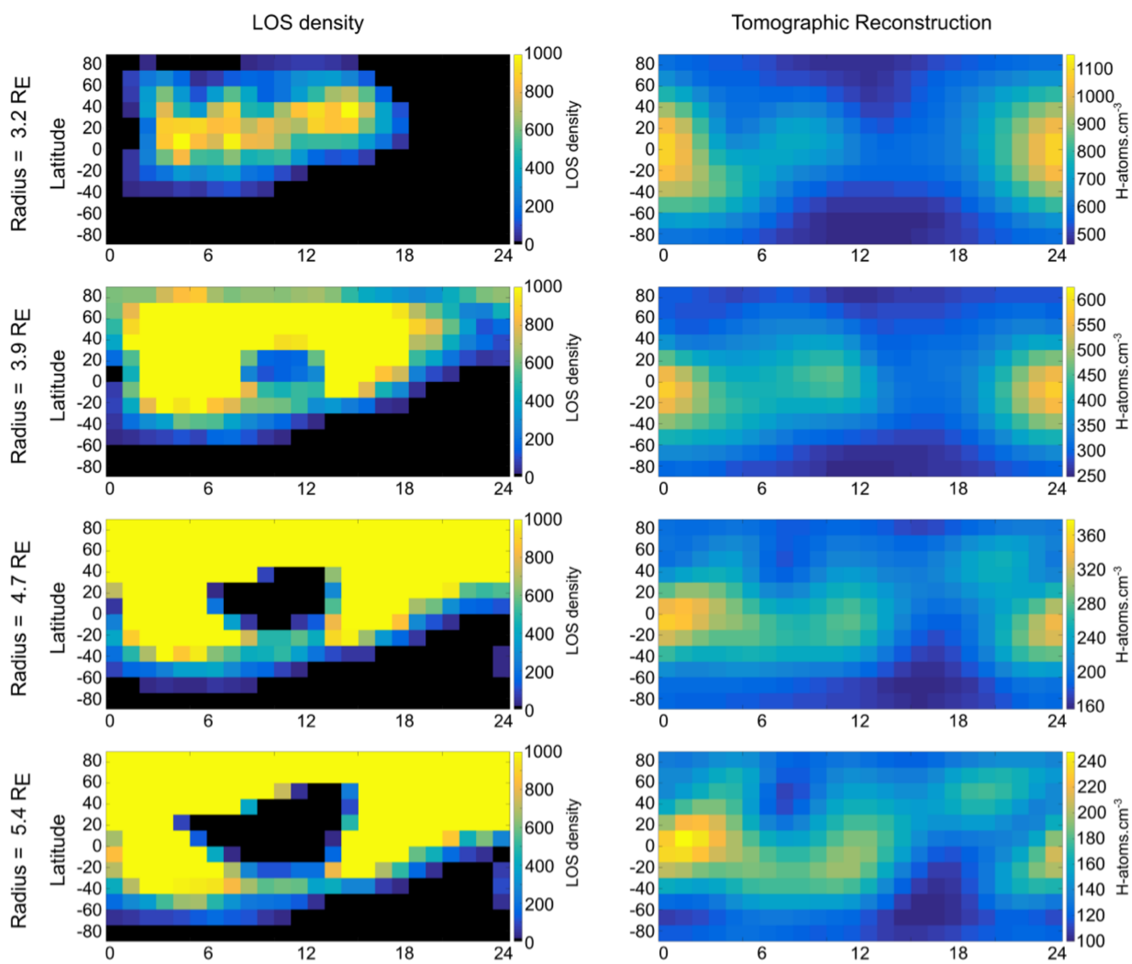

◉ Dynamic tomographic reconstruction during the storm occurred on March 17, 2013 [Cucho-Padin & Waldrop, 2019 (https://doi.org/10.1029/2019GL084327)].

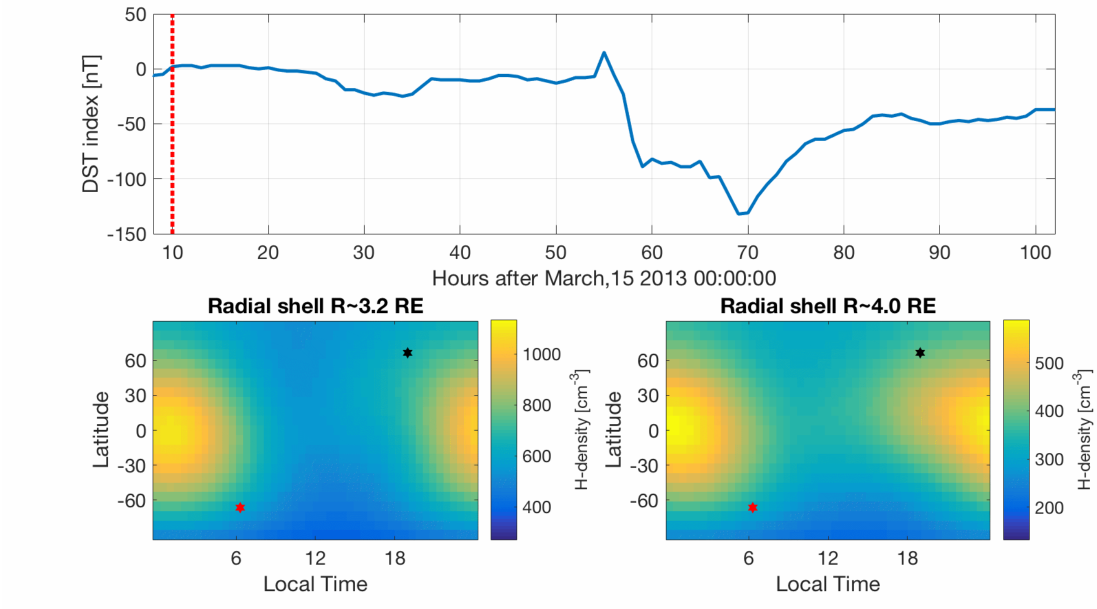

◉ Temporal evolution of the H density for selected spatial locations.

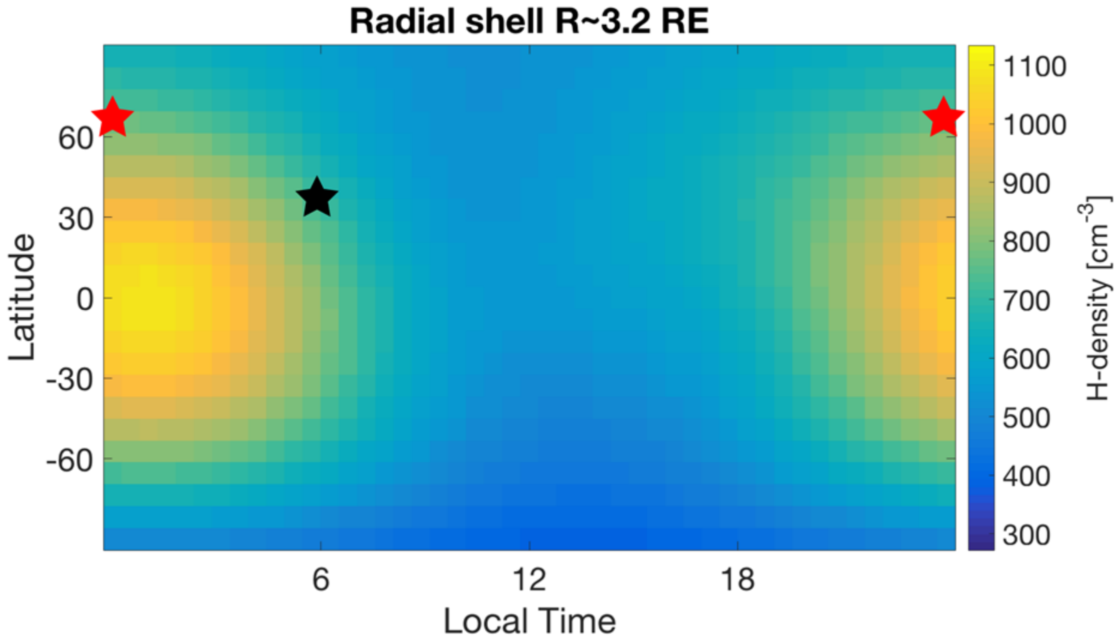
Radial shell R~3.2 RE
Latitude
60
30
0
-30
-60
6
12
18
Local Time
H-density [cm^{-3}]
1100
1000
900
800
700
600
500
400
300

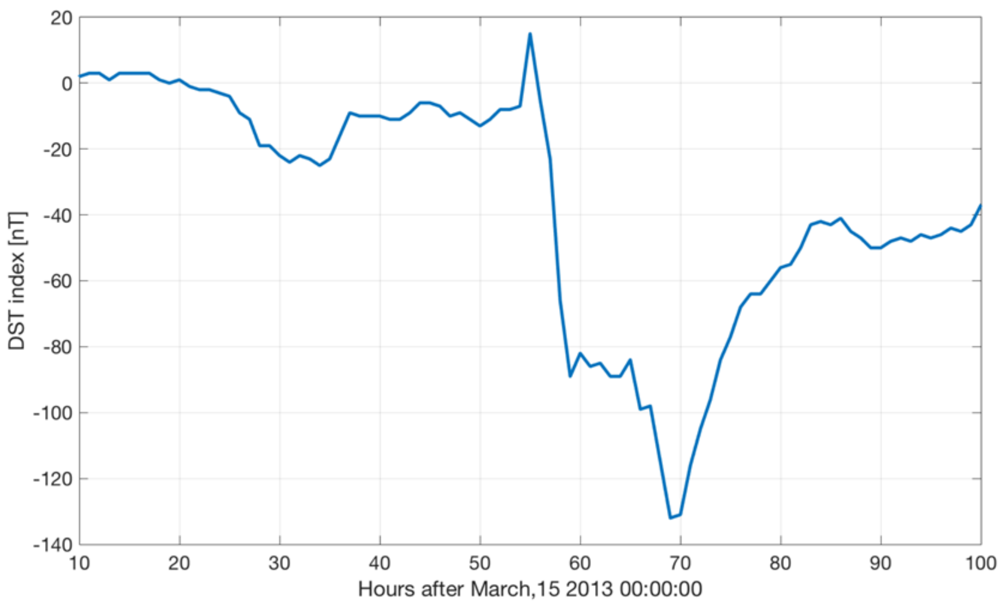
DST index [nT]
20
0
-20
-40
-60
-80
-100
-120
-140
10
20
30
40
50
60
70
80
90
100
Hours after March,15 2013 00:00:00

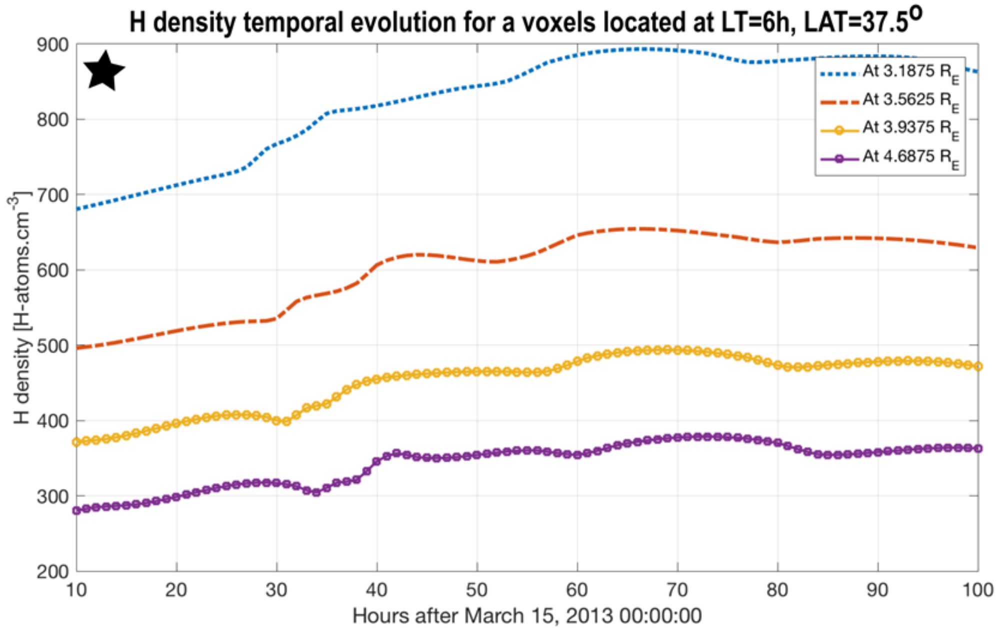

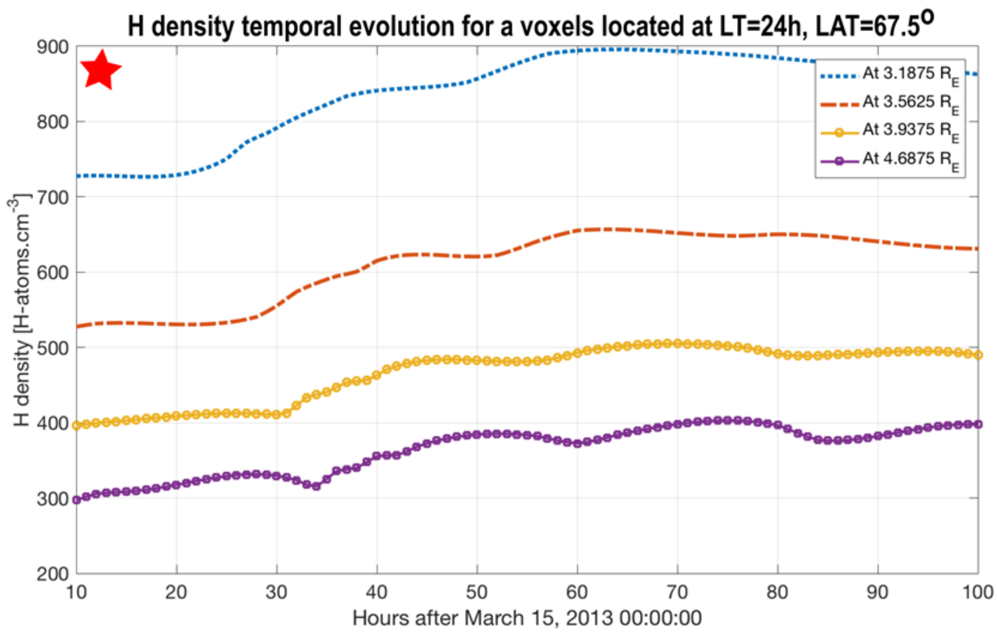

Highlights

✓ The temporal evolution of the H density shows a **~23%** increment (at the peak ~70h after March 15) with respect to quiet-time.

✓ Analysis of H density at different altitudes shows an **outward propagation** of H atoms.

✓ A constant increment of H density starting at ~30h after March 15 reveals that even **small geomagnetic variations** (DST~ -30nT) can trigger an increased H escape.

✓ The balance of injection and loss of H atoms in this region is affected by **exosphere-plasmasphere interaction and thermospheric variations** [Kuwabara et al., 2017 (https://agupubs.onlinelibrary.wiley.com/doi/full/10.1002/2016JA023247)]

IV. SIMULATIONS OF THE PLASMASPHERE DURING STORM-TIME

Incorporating the dynamic H profile into the IPE model

◉ We analyze the plasmaspheric refilling rate using the H density profile obtained by NRL MSIS-00 and our dynamic H density derived from Ly-α emission (TWINS/GUVI).

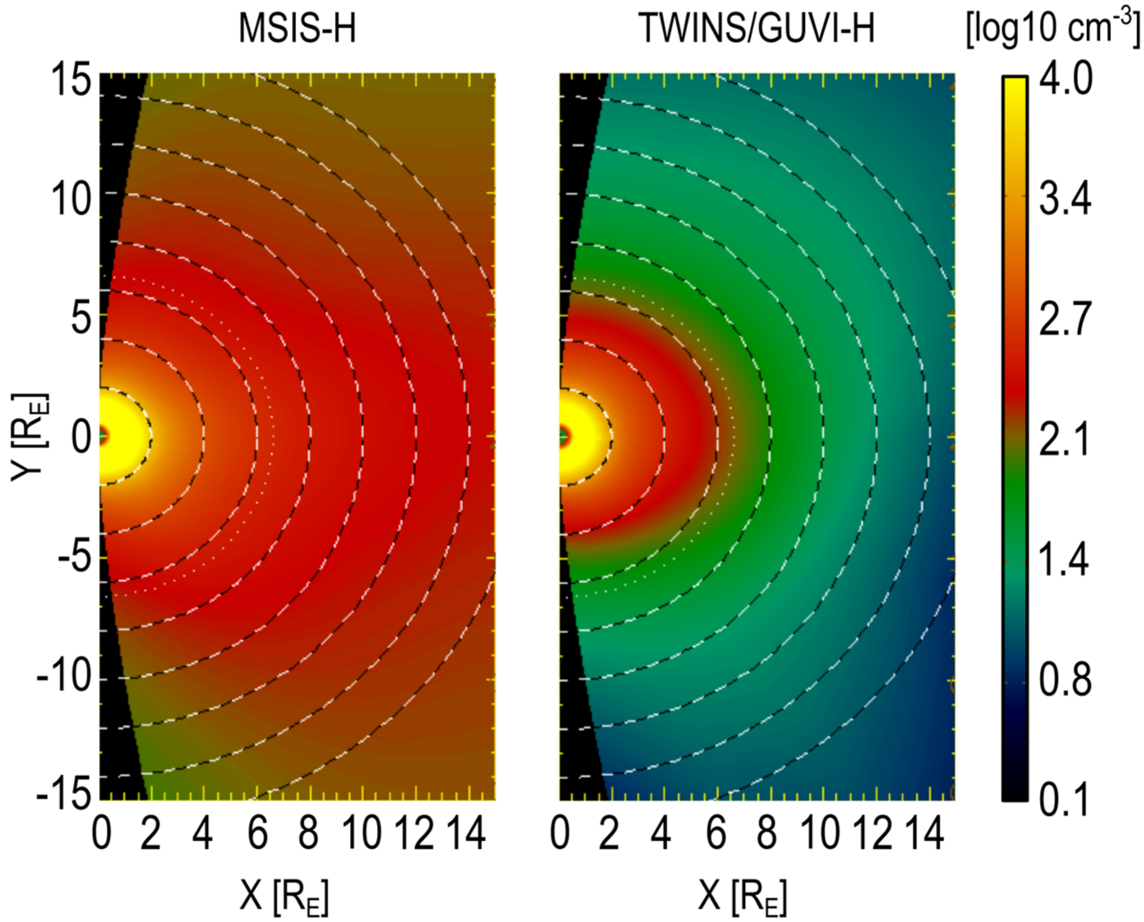

◉ IMF Bz, By, solar wind speed Vsw, and density Nsw measured from the ACE satellite, and DST, SYM-H on **17-18 March 2013**.

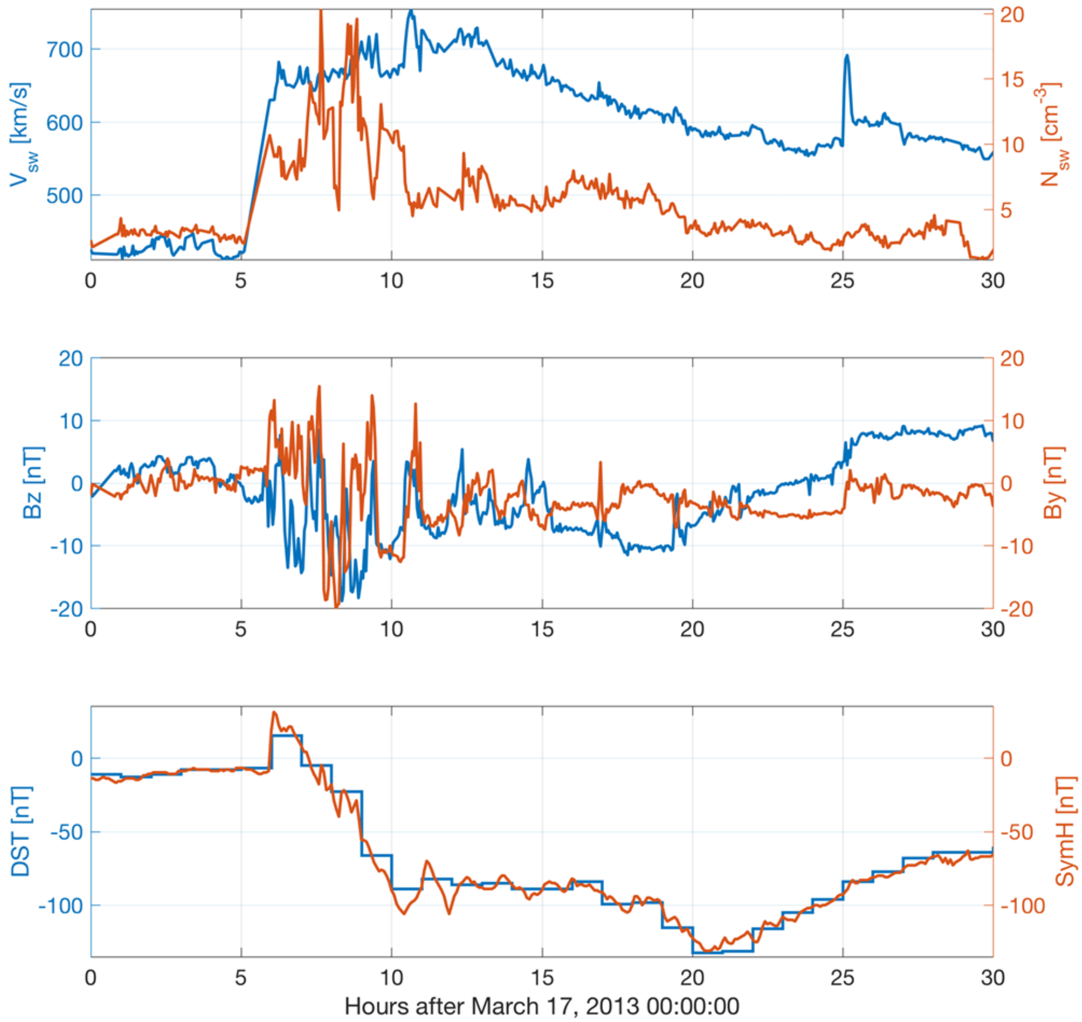

◉ Refilling rate comparison for two different solar conditions.

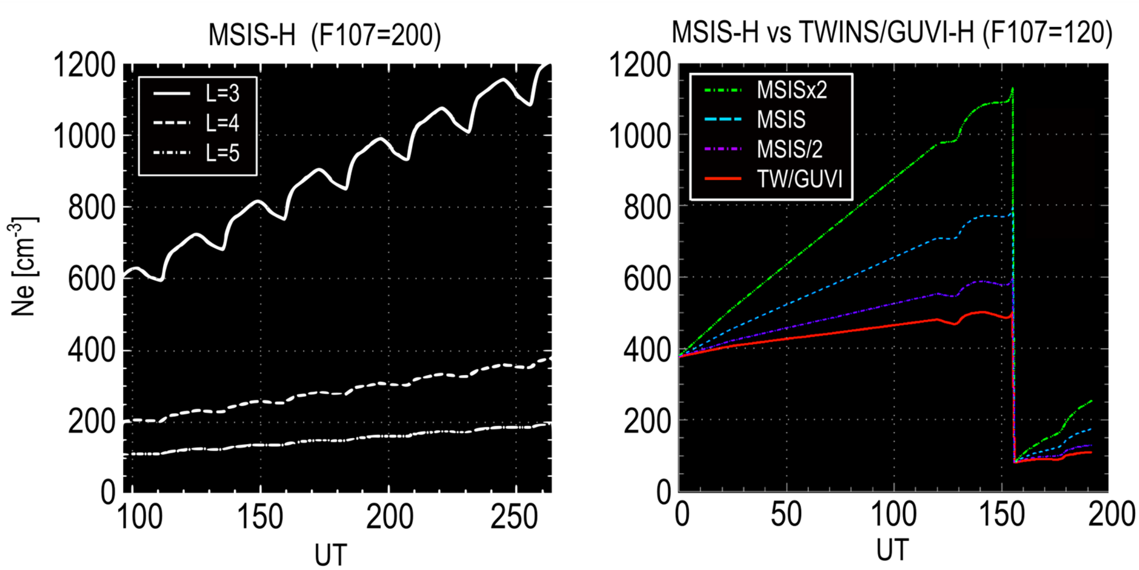

The left panel shows the refilling recovery using MSIS H density profile for simulated conditions with F107=200. The lines show the temporal evolution of the electron density of a flux tube at L=3,4,5 in the American longitude sector.

◉ Comparison of ion profiles at L=4 and LT=12h with both MSIS and TW/GUVI H density profiles.

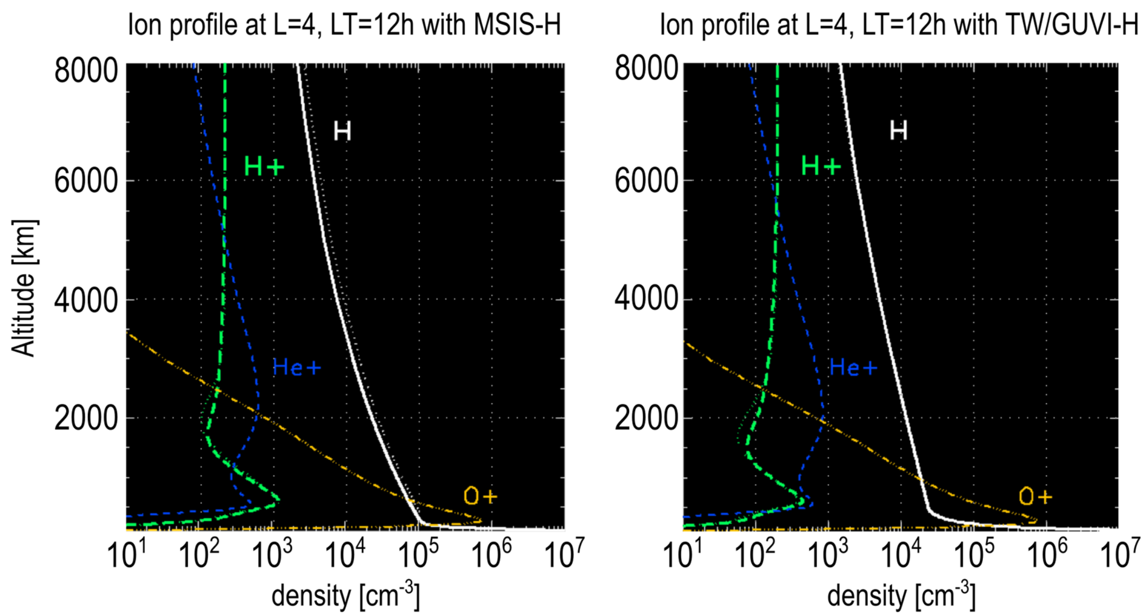

Highlights

✓ Refilling rates identified for default case are:

- L=3 : 89.4 [cm^{-3}.d^{-1}]
- L=4 : 25.4 [cm^{-3}.d-^{1}]
- L=5 : 12.2 [cm^{-3}.d^{-1}]

✓ Refilling rates identified during March 17, 2013 storm:

- MSISx2 : 99.0 [cm^{-3}.d^{-1}]
- MSIS : 53.3 [cm^{-3}.d-^{1}]
- MSIS/2 : 27.2 [cm^{-3}.d^{-1}]
- TW/GUVI : 19.4 [cm^{-3}.d^{-1}]

V. REFILLING RATE COMPARISON

◉ Our refilling rates have good agreement with those reported in [Denton et al., 2012]

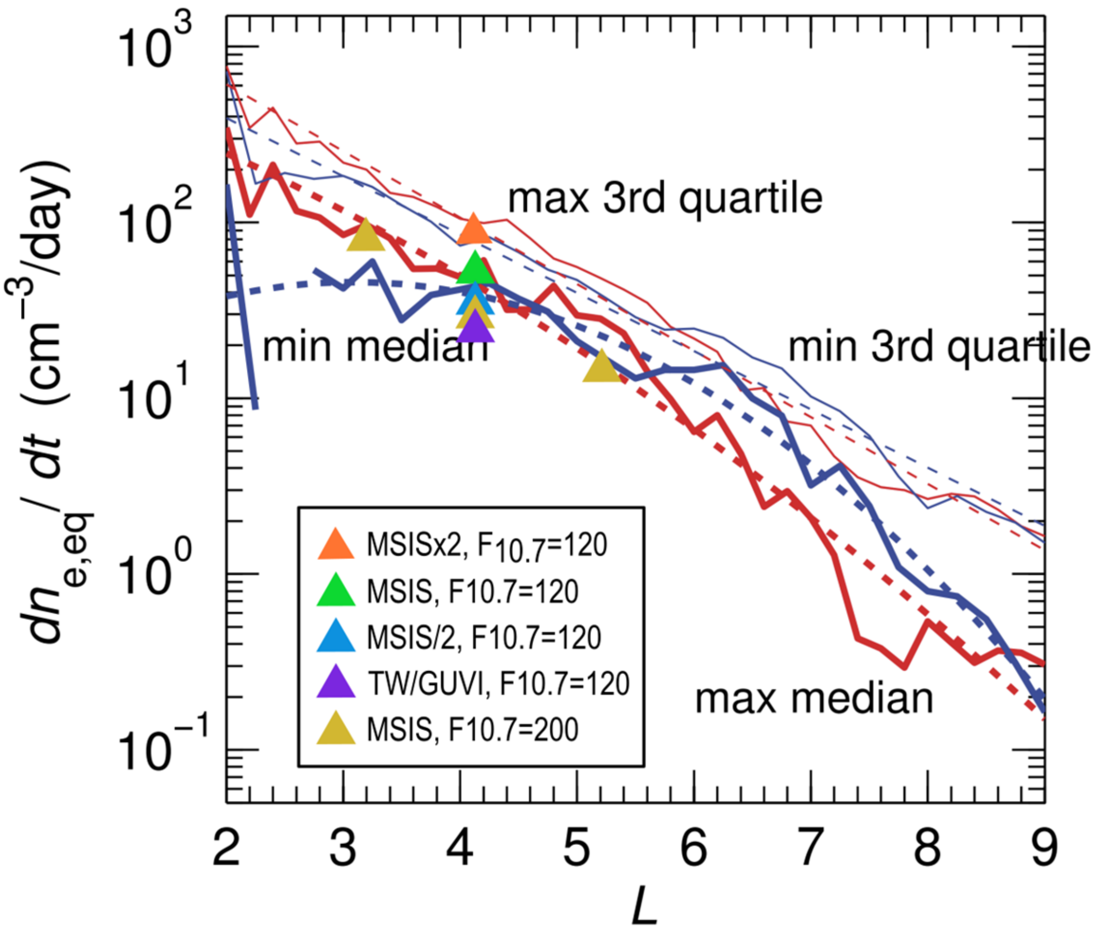

Median (thick solid curves) and third quartile (thin solid curves) for the refilling rate $dn_{e,eq}/dt$ during intervals corresponding to solar maximum (red curves) and solar minimum (blue curves). The dotted curves are the corresponding quadratic fits described in the text.

VI. CONCLUSIONS

Conclusions

✓ In this work, we have developed a technique to estimate time-dependent H density from its Ly-α emission. The H density profile has been used to analyze the refilling rate in the plasmasphere during storm-time.

✓ These results emphasize the importance of an accurate estimation of exospheric H density and the need for satellite-based missions to specifically measure the exosphere. The Global Lyman-alpha Imagers for the Dynamic Exosphere (GLIDE) mission led by Dr. Waldrop, has been accepted for launch in 2024. It will provide wide-field global images of the exosphere with a 30-min temporal resolution.

ABSTRACT

As soon as the outer plasmasphere gets eroded during geomagnetic storms, the greatly depleted plasmasphere is replenished by cold, dense plasma from the ionosphere. A strong correlation has been revealed between plasmaspheric refilling rates and ambient densities in the topside ionosphere and exosphere, particularly that of atomic hydrogen (H). Although measurements of H airglow emission at plasmaspheric altitudes exhibit storm-time response, temporally static distributions have typically been assumed in the H density in plasmasphere modeling. In this presentation, we evaluate the impact of a realistic distribution of the dynamic H density on the plasmaspheric refilling rate during the geomagnetic storm on March 17, 2013. The temporal and spatial evolution of the plasmaspheric density is calculated by using the Ionosphere-Plasmasphere Electrodynamics (IPE) model, which is driven by a global, 3-D, and time-dependent H density distribution reconstructed from the exospheric remote sensing measurements by NASA's TWINS and TIMED missions. We quantify the spatial and temporal scales of the refilling rate and its correlation with H densities.

REFERENCES

Krall, J., Glocer, A., Fok, M.−C., Nossal, S. M., & Huba, J. D. (2018). The unknown hydrogen exosphere: Space weather implications. Space Weather, 16, 205– 215. https://doi.org/10.1002/2017SW001780

Bailey, J., and Gruntman, M. (2011), Experimental study of exospheric hydrogen atom distributions by Lyman−alpha detectors on the TWINS mission, J. Geophys. Res., 116, A09302, doi:10.1029/2011JA016531.

Zoennchen, J. H., et al. (2015) "Terrestrial exospheric hydrogen density distributions under solar minimum and solar maximum conditions observed by the TWINS stereo mission." Annales Geophysicae, vol. 33, no. 3, p. 413.

Hodges, R. R. (1994), Monte Carlo simulation of the terrestrial hydrogen exosphere, J. Geophys. Res., 99(A12), 23229-23247, doi:10.1029/94JA02183.

Zoennchen, J. H., Nass, U., Fahr, H. J., and Goldstein, J.: The response of the H geocorona between 3 and 8 Re to geomagnetic disturbances studied using TWINS stereo Lyman-α data, Ann. Geophys., 35, 171–179, https://doi.org/10.5194/angeo-35-171-2017, 2017.

Kuwabara, M., Yoshioka, K., Murakami, G., Tsuchiya, F., Kimura, T., Yamazaki, A., and Yoshikawa, I. (2017), The geocoronal responses to the geomagnetic disturbances, J. Geophys. Res. Space Physics, 122, 1269– 1276, doi:10.1002/2016JA023247.

McComas, D.J., Allegrini, F., Baldonado, J. et al. (2009) The Two Wide-angle Imaging Neutral-atom Spectrometers (TWINS) NASA Mission-of-Opportunity. Space Sci Rev 142, 157–231. https://doi.org/10.1007/s11214-008-9467-4

Qin, J., Waldrop, L., and Makela, J. J. (2017), Redistribution of H atoms in the upper atmosphere during geomagnetic storms, J. Geophys. Res. Space Physics, 122, 10,686– 10,693, doi:10.1002/2017JA024489.

Østgaard, N., Mende, S. B., Frey, H. U., Gladstone, G. R., and Lauche, H. (2003), Neutral hydrogen density profiles derived from geocoronal imaging, J. Geophys. Res., 108, 1300, doi:10.1029/2002JA009749, A7.

Cucho−Padin, G., & Waldrop, L. (2018). Tomographic estimation of exospheric hydrogen density distributions. Journal of Geophysical Research: Space Physics, 123, 5119– 5139. https://doi.org/10.1029/2018JA025323

Cucho−Padin, G., & Waldrop, L. (2019). Time−dependent response of the terrestrial exosphere to a geomagnetic storm. Geophysical Research Letters, 46, 11661– 11670. https://doi.org/10.1029/2019GL084327

Rairden, R. L., Frank, L. A., and Craven, J. D. (1986), Geocoronal imaging with Dynamics Explorer, J. Geophys. Res., 91(A12), 13613– 13630, doi:10.1029/JA091iA12p13613.